

Study of acid-base balance in the soil-groundwater system

O.A. Khakhel¹, T.P. Romashko², 2026

¹Poltava Gravimetric Observatory of S. Subbotin Institute
of Geophysics of National Academy of Sciences of Ukraine, Poltava, Ukraine

²Poltava State Agrarian University, Poltava, Ukraine

Received 12 March 2026

The interaction between pH-buffer systems of soil and groundwater may play a role in shaping the hydrogeochemical conditions that affect pH stability in these two environments. Despite extensive studies of soil and groundwater, the related behavior of these systems remains poorly understood, especially under conditions of spatial heterogeneity and anthropogenic influence. This study aims to investigate the interaction between soil pH-buffering mechanisms and groundwater chemistry, focusing on identifying the dominant processes governing pH regulation. We measured pH, total alkalinity, calcium ion concentrations, and components of the carbonate buffer system. Soil and groundwater exhibited an interrelated buffering mechanism. pH stabilization in the studied system was controlled by the combined effect of multiple buffering mechanisms, including mineral equilibria, ion exchange, and solution-phase reactions. These processes operated in a coupled manner and were influenced by hydrodynamic conditions and local environmental factors. A conceptual model of «collective buffering action» is proposed to describe the integrated effect of interacting buffering processes, whereby soils and groundwater function as an integrated acid-base system. The model is intended as a qualitative framework rather than a fully quantitative representation. Three phases of buffer interaction between soil and groundwater were identified, ranging from background equilibrium to developed alkalization or acidification, with opposite or synchronized shifts in the pH of soil and groundwater depending on the phase. This mechanism can give early warnings of acid-base disturbances and has practical implications for hydrological environmental monitoring.

Key words: soil pH, groundwater pH, pH-buffers interaction.

Introduction. The pH of an environmental medium is a fundamental parameter that governs its physical, chemical, and biological processes. In natural settings, soil and groundwater are in direct contact; however, the extent to which they influence each other's pH remains poorly understood. Some studies have investigated soil [Nelson, Su, 2010; Fabian et al., 2014; Luo et al., 2015; Slesarev et al., 2016] or groundwater pH [Hájek et al., 2021; Klaus, 2023] across large areas and examined their spatial patterns. Such works aim to clarify a wide range of issues, includ-

ing the relationship between environmental pH and lithology, climate, past glaciations, etc. However, the potential interactions between soil and groundwater have not been addressed.

In this study, we compared pH values measured in groundwater and in the corresponding overlying soil profiles at several locations across an area of approximately 15×40 km. The results revealed a relationship between soil and groundwater pH. This observation prompted further investigation into the underlying mechanisms influencing environ-

Citation: Khakhel' O.A., & Romashko T.P. (2026). Study of acid-base balance in the soil-groundwater system. *Geofizychnyi Zhurnal*, 48(3), 103—111. <https://doi.org/10.24028/gj.v48i3.354142>.

Publisher Subbotin Institute of Geophysics of the NAS of Ukraine, 2026. This is an open access article under the CC BY-NC-SA license (<https://creativecommons.org/licenses/by-nc-sa/4.0/>).

mental pH, which are discussed in this work.

Study area and sampling design. Field investigations were conducted in the Poltava region of Ukraine, within a zone dominated by podzolized chernozem soils. The sampling locations are shown in Fig. 1. Groundwater and soil samples were collected during two field campaigns: the first in December 2020 and the second in July 2021.



Fig. 1. Soil and groundwater sampling sites (with the base layer extracted from ©Google Maps). The numbers 1 to 16 indicate the numbers of the locations where the samples were taken.

Groundwater and soil sampling. Groundwater samples were obtained from domestic wells on the plots with water table depths ranging from 3 to 18 m. All samples were analyzed within 24 hours of collection.

Soil samples were collected from a depth of 10–25 cm on fallow lands that had not been cultivated for more than 10 years. The horizontal distance between soil and groundwater sampling points ranged from 15 to 100 m.

Preparation of soil aqueous extracts. Soil samples were dried at 40 °C, homogenized, and sieved through a 2 mm mesh. Aqueous extracts were prepared by mixing soil with deionized water at a 1:2.5 (w/v) ratio. Suspensions were equilibrated for 24 hours at room temperature and subsequently filtered through cellulose filters prior to analysis.

Measurements. The pH of groundwater and soil aqueous extracts was determined using a calibrated I-160MI ionometer equipped with ES-10603 glass and ESr-10103 reference electrodes. Calibration was performed using standard buffer solutions (pH 4.01, 6.86, and 9.18). The instrumental measurement uncertainty was ± 0.03 pH units.

Determination of total alkalinity and calcium ion concentrations. Since the measured pH values of both groundwater and soil extracts were within the the $\text{HCO}_3^-/\text{CO}_2$ system's buffering capacity, additional parameters were evaluated to examine the pH-regulation mechanisms. Specifically, the total alkalinity (TA) and calcium ion (Ca^{++}) were measured to quantify the carbonate equilibrium. They were determined by titration in four analytical replicates.

TA was measured by acid-base titration using $0.05 \text{ mol} \cdot \text{l}^{-1}$ HCl. The endpoint was determined using a mixed indicator composed of methyl red and bromocresol green, appropriate for detecting buffering systems in natural waters. The concentration of TA (in $\mu\text{mol} \cdot \text{l}^{-1}$) was calculated using the formula: $\text{TA} = C_{\text{HCl}} V_{\text{HCl}} 1000 / V_{\text{sample}}$, where C_{HCl} is the concentration of the acid ($\text{mol} \cdot \text{l}^{-1}$), V_{HCl} is the volume of acid used for titration (ml), and V_{sample} is the volume of the sample (ml).

Calcium concentration was determined by complexometric titration with $0.05 \text{ mol} \cdot \text{l}^{-1}$

disodium ethylenediaminetetraacetic acid (EDTA) using murexide as a colorimetric indicator. The concentration of calcium (in $\mu\text{mol}\cdot\text{l}^{-1}$) was calculated according to the equation: $\text{Ca}^{++} = C_{\text{EDTA}} V_{\text{EDTA}} 1000 / V_{\text{sample}}$, where C_{EDTA} is the molar concentration of the EDTA solution ($\text{mol}\cdot\text{l}^{-1}$), V_{EDTA} is the volume of EDTA used (ml), and V_{sample} is the volume of the sample (ml).

All titrations were performed at a constant laboratory temperature of 25 ± 0.5 °C. Relative analytical uncertainty was below 5 %.

Calculations of carbonate buffer parameters. A carbonate buffer system can be fully characterized by measuring any two of four parameters: partial pressure CO_2 , TA, pH, and dissolved inorganic carbon. In this study, bicarbonate (HCO_3^-) and dissolved carbon dioxide concentrations were calculated from measured pH and TA values using the freshwater carbonate system algorithm of [Lewis, Wallace, 1998].

Because the aquifer contains limestone, the carbonate equilibrium is influenced by mineral buffering. Furthermore, due to CO_2 , 's

high mobility and volatility, its measured concentrations in groundwater may deviate from equilibrium conditions. To account for this, equilibrium CO_2 concentrations were calculated from calcium and bicarbonate concentrations according to the classical carbonate equilibrium expression: $[\text{CO}_2] = [\text{Ca}^{++}] [\text{HCO}_3^-]^2 / K_{\text{CO}_2}$, where K_{CO_2} is the equilibrium constant for dissolved CO_2 in water [Stumm, Morgan, 1996]. For groundwater at 9 °C, the value of K_{CO_2} was adopted as $3.45 \cdot 10^{-5}$, based on the data of Plummer and Busenberg [Plummer, Busenberg, 1982].

Results. The results of pH measurements in groundwater and soil samples, groundwater depths, TA values, and calcium ion contents are summarized in the Table. One might expect a direct relationship between groundwater and overlying soil pH, but correlation analysis showed that a negative relationship could also be observed between these two variables. As illustrated in Fig. 2, a, pH values at sites 1 and 4 deviate strongly from the background cluster formed by sites 2, 3, and 5, resulting in a pronounced negative regression.

Physicochemical parameters of soil and groundwater at the sampling sites (July 2021)

Sampling site ¹	Groundwater			Aqueous soil extract	
	pH	TA, $\mu\text{mol}\cdot\text{l}^{-1}$	Ca^{++} , $\mu\text{mol}\cdot\text{l}^{-1}$	pH	TA, $\mu\text{mol}\cdot\text{l}^{-1}$
1 (15 m)	7.20 (7.01) ²	8375	3350	7.54 (7.60) ²	1250
2 (15 m)	7.42 (7.37) ²	7250	3150	7.38 (7.24) ²	1750
3 (7 m)	7.36 (7.45) ²	8625	2650	7.31 (7.20) ²	1650
4 (7 m)	7.35 (7.70) ²	7375	2500	7.29 (6.94) ²	1125
5 (12 m)	7.33 (7.43) ²	7375	2600	7.39 (7.25) ²	1950
6 (4 m)	7.30	6375	3000	7.32	875
7 (13 m)	7.33	7125	2750	7.45	1950
8 (12 m)	7.35	7125	2600	7.30	2500
9 (7 m)	7.37	9375	2500	7.34	1750
10 (13 m)	7.41	8875	2600	7.43	1250
11 (9 m)	7.27	9875	3250	7.48	1050
12 (18 m)	7.17	6625	3625	7.60	1550
13 (10 m)	7.21	8630	2250	7.60	2250
14 (13 m)	7.42	7375	2000	7.67	1750
15 (13 m)	7.06	10125	3050	7.45	2100
16 (3 m)	6.85	5625	3700	7.20	1050

Notes: ¹The sampling sites are numbered according to the map shown in Fig. 1. Groundwater depths at each site are provided in parentheses; ²Values in parentheses correspond to data obtained during the December 2020 sampling campaign.

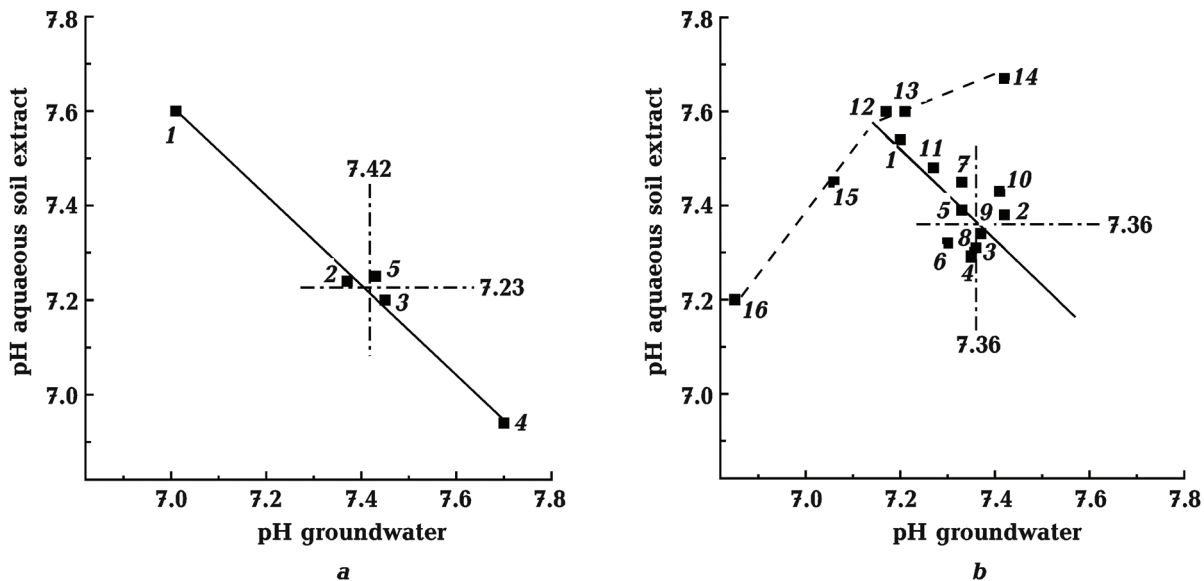


Fig. 2. pH values of soil aqueous extracts and groundwater at the sampling sites, measured in December 2020 (a) and July 2021 (b). Site numbers correspond to those shown in Fig. 1.

Fig. 2, a presents the data obtained during the winter sampling campaign. Repeated measurements were taken in the summer of 2021, with the network of observation points expanded. The results of the summer pH measurements are presented in Fig. 2, b. These data demonstrate a more complex relationship between soil and groundwater pH values, but for sites 1—12, the analysis still reveals a statistically significant negative correlation.

The focus of this study is on the mechanism underlying the observed relationship between soil and groundwater pH. We propose that soil and groundwater constitute a coupled system of pH buffers that interact through ion-exchange processes occurring within the unsaturated zone, as discussed below.

Discussion. The defining property of any buffer solution is its buffer capacity, which reflects its ability to resist pH changes within a certain range of added acids or bases. Consider dividing such a solution into two parts by some interface — for example, a membrane — that provides electrochemical contact between the two subsystems thus formed (designated as subsystems I and II). In this case, the overall buffer capacity of the

initial solution will be distributed effectively between the subsystems, and their pH values (pH_I and pH_{II}) will generally differ, depending on the membrane properties. When acids or bases are introduced into subsystem I or II, the relationship between pH_I and pH_{II} can be expressed as $d\text{pH}_I/d\text{pH}_{II} = f(x)$, where x is a factor influencing the acid-base balance in the system, and $f(x)$ is a function determined by the properties of the membrane. If the membrane is permeable to the added substances, then the pH_I and pH_{II} will change in the same direction, i.e., $f(x)$ is positive. However, if the membrane is impermeable to the added species but still allows interrelated reactions to occur in both subsystems, $f(x)$ may take negative values.

Indeed, if an initial buffer solution of pH_0 is divided into two subsystems separated by an ion-permeable barrier, and an acid or base is added to one subsystem in an amount that exceeds its individual buffer capacity but not that of the original solution, then pH_I and pH_{II} will shift in opposite directions, preserving the integrity of the buffering capacity of the entire system, since upon removal of the partition the solution obtained in such an experiment will restore to its original pH_0 . This reasoning implies that two linked buffers

can act in a coordinated manner to maintain a generalized common pH level (pH_Σ), which can be referred to as collective buffering action. The behavior of such a system can be approximated by equation, $\text{pH}_\Sigma = \text{pH}_I + a\text{pH}_{II}$, obtained by integrating the differential relationship above, where $a = -f(x)$. The range in which pH_Σ and a remain stable defines the collective buffer capacity of the system.

If the addition of acid or base exceeds the buffering capacity of the initial solution, both pH_I and pH_{II} will begin to shift in the same direction.

Based on this framework, three phases of buffers' interaction can be distinguished:

- initial equilibrium phase, where the system is separated by an electrochemical barrier, resulting in the difference $\Delta\text{pH} = \text{pH}_I - \text{pH}_{II}$ determined by the membrane properties;
- reciprocal adjustment phase, in which the buffering capacity of one subsystem is exceeded, while that of the whole system is not; pH values shift in opposite directions;
- saturation phase, where buffering capacities of the initial solution are exceeded, resulting in unidirectional pH changes in both subsystems.

This model of interacting pH buffers appears straightforward for experimental testing under laboratory conditions; however, to the best of our knowledge, no such studies have been reported in the literature. Apparently, the obstacle to conducting such an experiment is the lack of a suitable membrane for separating the buffer solution.

Understandably, in real-world systems such as soil and groundwater, the interactions between buffers differ from the simplified model described above. Unlike isolated laboratory systems, groundwater and soil are open and dynamic. Nevertheless, when their buffering capacities are combined, a pH response analogous to the modeled behavior can be expected in response to disturbances in the acid-base balance. Moreover, their contact can be ensured by nothing other than a capillary-pore network extending, as is known [Hillel, 2004], through the vadose

zone. In this context, it should be emphasized that capillary osmosis and ion selectivity in porous membranes are well-established concepts [Sasidhar, Ruckenstein, 1981]. However, applying these principles directly to soil substrates has inherent limitations. Even so, this porous medium provides the necessary electrochemical contact between soil and groundwater, most likely mediated by the transfer of highly mobile ions in vapor form.

Let us now analyze the data presented in Fig. 2 in light of the proposed model of soil-groundwater buffer interaction. From Fig. 2, *a*, it can be seen that sites 2, 3, and 5 form a separate cluster with closely similar pH values: soil pH ranges from 7.20 to 7.25 (mean 7.23), while groundwater pH ranges from 7.37 to 7.45 (mean 7.42). These average values obviously correspond to the background pH values for the studied subregion. If pH_I is the pH of groundwater and pH_{II} is the pH of soil, the difference $\Delta\text{pH}_{I,II} \approx 0.2$ indicates the presence of an effective buffer interface. This offset is independent of groundwater depth, highlighting the role of ion mobility in establishing electrochemical equilibrium. A linear approximation of the data in Fig. 2, *a*, yields the following relationship: $14.21 = \text{pH}_I - 0.94\text{pH}_{II}$.

The anomalies observed at sites 1 and 4 (see Fig. 2, *a*) are unlikely to result from changes in the ion-selective properties of the substrate. Rather, they suggest the influence of external factors — such as anthropogenic activities or local environmental conditions — that have disrupted the buffering equilibrium.

While Fig. 2, *a*, contains data corresponding only to the first and second phases of buffer interaction, Fig. 2, *b*, captures all three phases. Sites representing background conditions (2—10) fall within a circle of 0.16 pH unit diameter, which provides an estimate of the natural equilibrium variance. The mean background pH values measured in summer are nearly identical for soil and groundwater (~ 7.36), resulting in $\Delta\text{pH}_{I,II} \approx 0$, compared with $\Delta\text{pH}_{I,II} \approx 0.2$ in winter. This seasonal shift may reflect temperature-dependent modulation of the system. Groundwater temperature remains relatively stable throughout the year ($\sim 9^\circ\text{C}$), whereas soil temperature varies by

over 30 °C between seasons. This thermal gradient likely alters the ion permeability of the clay-rich layer separating soil and groundwater, thereby influencing $\Delta\text{pH}_{\text{I,II}}$. The fact that the increase in soil pH (from 7.23 to 7.36) exceeds the corresponding decrease in groundwater pH (from 7.42 to 7.36) from winter to summer is consistent with this interpretation.

The summer data in Fig. 2, *b* for sites 1, 11, and 12 indicate a manifestation of the second interaction phase between soil and groundwater pH buffers. Focusing on sites 1—12 — classified as belonging to phases one and two, the summer dataset, like the winter dataset, demonstrates a linear relationship with a regression line slope close to -1 : $14.39 = \text{pH}_{\text{I}} - 0.95\text{pH}_{\text{II}}$.

As shown, the overall pH dynamics remain relatively stable across seasons, although some differences are evident. In addition to the seasonal shift in $\Delta\text{pH}_{\text{I,II}}$, there is also a seasonal narrowing of the pH range within which the soil-groundwater system operates during the second phase of buffering interaction; this range is broader in winter but becomes more restricted in summer.

Another difference concerns the pH behavior at site 4. The deviation from background values recorded in winter 2020 (see Fig. 2, *a*), which was absent in summer 2021, is most likely attributable to a natural geochemical process rather than seasonality. The point is

that the study area lies within a geochemical province containing a Paleogene aquifer with fluoride-rich, alkaline artesian waters [Zhovinsky et al., 2001]. The winter pH data suggest an episode of upward discharge from this artesian aquifer altering the groundwater chemistry and consequently disturbing the overlying soil buffer system at site 4. By summer 2021, this anomaly had disappeared (see Fig. 2, *b*), undoubtedly due to dilution by local groundwater recharge. This supports the assumption that the interaction between soil and groundwater pH buffers occurs through the exchange of volatile ions, without the transfer of alkalinizing or acidifying agents.

The third phase of buffer interaction is seen at sites 13—16. At that, at sites 13, 14 and 15, 16, the pH values shift in different directions, as shown by the dashed lines in Fig. 2, *b*. This indicates that the system disturbances differ in origin, that is, the disruption of the soil-groundwater pH balance may arise from one of four scenarios:

- soil alkalization, in the early stages, causing groundwater acidification;
- soil acidification, in the early stages, causing groundwater alkalization;
- groundwater alkalization, in the early stages, causing soil acidification;
- groundwater acidification, in the early stages, causing soil alkalization.

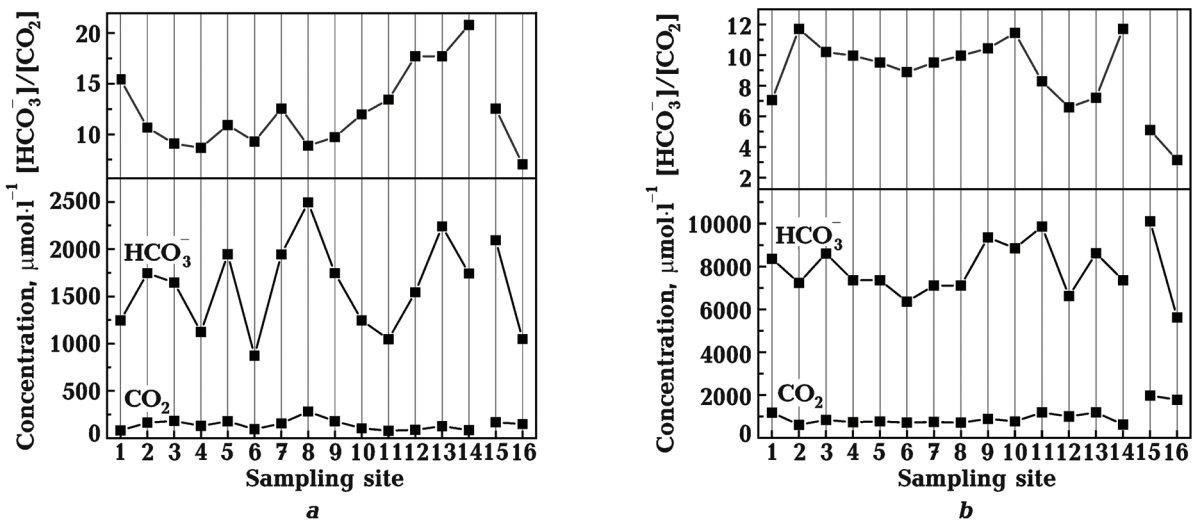


Fig. 3. Concentrations of bicarbonate and carbon dioxide in soil aqueous extracts (*a*) and groundwater (*b*), calculated from pH and TA values measured in July 2021. Sampling site numbers correspond to those shown in Fig. 1.

To identify which of these scenarios occurred in the studied system, we analyzed the behavior of the components of soil and groundwater pH buffers. We analyzed HCO_3^- and CO_2 concentrations in groundwater and soil aqueous extracts collected in July 2021. The results are presented in Fig. 3.

Data from sites 15 and 16 are shown separately from the main group in Fig. 3 because they share a distinct cause of pH disturbance compared to the other sites. At both locations, deviations from background values are due to groundwater acidification. At site 15, the acidification is most likely of anthropogenic origin, caused by sewage contamination. At site 16, the process appears natural: the site is located approximately 100 m from the bank of the Serednia Hovtva River, a small, swampy river with subacidic water. The seepage from the river into the shallow groundwater horizon likely acidifies the latter.

In contrast, at sites 1 and 11–14, the observed disturbances arise from soil alkalization. Here, a progression can be traced from background conditions to increasingly pronounced soil alkalization, accompanied by a corresponding groundwater response.

Thus, when soil undergoes alkalization, its pH stability is maintained through bicarbonate dissociation. Alkalization reduces the CO_2 content of soil water; the bicarbonate concentration subsequently decreases in proportion, while the $[\text{HCO}_3^-]/[\text{CO}_2]$ ratio remains nearly constant. According to the Henderson-Hasselbalch equation, this constancy ensures relative pH stability. This behavior is clearly seen at sites 2–10, where soil and groundwater pH values remain stable and $[\text{HCO}_3^-]/[\text{CO}_2]$ ratios show little variation. These sites, therefore, represent the first phase of buffering equilibrium, characterized by minimal external disturbance. Slight deviations at sites 7 and 10 (see Fig. 3, a) may indicate the very onset of soil alkalization, though no clear groundwater response is yet evident.

At sites 1, 11, and 12, the soil shows a marked increase in the $[\text{HCO}_3^-]/[\text{CO}_2]$ ratio (see Fig. 3, a), accompanied by higher soil pH. In groundwater at the same sites, however,

the $[\text{HCO}_3^-]/[\text{CO}_2]$ ratio decreases and pH declines (see Fig. 3, b). This pattern demonstrates that the groundwater buffer responds in the opposite direction to soil processes, a hallmark of the second phase of buffer interaction, in which the buffer capacity of one subsystem (soil) is exceeded and the other (groundwater) compensates.

Sites 13 and 14 exemplify the third phase of soil-groundwater buffer interaction. Compared to site 12, both soil and groundwater show higher pH values (see Fig. 2, b), and the $[\text{HCO}_3^-]/[\text{CO}_2]$ ratio increases in both media (see Fig. 3). In this phase, the buffering capacities of both subsystems are exceeded, and their responses become unidirectional.

Additional data on groundwater pH, calcium, and carbon dioxide concentrations are presented in Fig. 4, providing further insight into the groundwater system's response to soil alkalization at sites 1 and 11–14.

The initiating factor in this response appears to be a reduction in soil H^+ ion concentration during the alkalization process. This perturbation disrupts the previously established proton equilibrium between soil and groundwater, creating a proton gradient that favors the migration of H^+ ions from

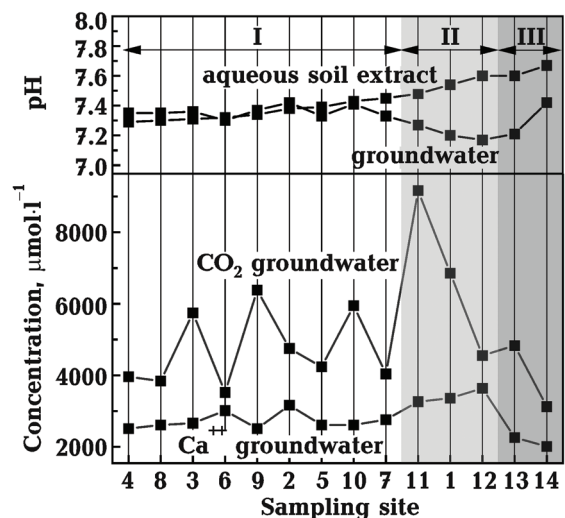


Fig. 4. Parameters of the groundwater buffer system at the sampling sites (see map in Fig. 1) as of July 2021. The sites are arranged in order of increasing pH of aqueous soil extracts. I, II, and III indicate the phases of interaction between soil and groundwater pH buffers.

groundwater into the soil. Such ion transfer compensates for the pH increase in the soil. Consequently, the partial pressure of H^+ in groundwater decreases, driving a shift in the groundwater buffering system toward reactions that regenerate H^+ ions. The initial response of the groundwater buffer is an increase in CO_2 concentration — the most labile component of the bicarbonate buffer — clearly observed at site 11 (see Fig. 4). This spike in CO_2 helps stabilize groundwater pH and, through a decrease in the $[HCO_3^-]/[CO_2]$ ratio, contributes to pH reduction. This change precedes observable shifts in more conservative parameters such as calcium concentration. As indicated by the data from sites 1 and 12–14, once the buffering capacity of groundwater is exhausted, CO_2 concentration begins to decline. This is subsequently followed — again with some delay — by an increase in groundwater pH and a reduction in total hardness.

The alkalization observed at sites 1 and 11–14 is, in our view, linked to the proximity of these locations to asphalted roads. It is known that asphalt can substantially alter soil chemistry and promote alkalization [Kida, Kawahigashi, 2015]. Moreover, the

long-term use of de-icing agents during winter road maintenance may further exacerbate this effect.

Conclusion. This study provides evidence that groundwater and soil moisture layers are not isolated systems but rather function as a single, integrated acid-base buffering complex. Their interaction is governed by ion-exchange processes within the vadose zone, which mediate reciprocal pH responses when the buffering capacity of either subsystem is challenged. At the early stage of disturbance, this manifests itself as a negative correlation between soil and groundwater pH. In contrast, at the later stage, once the collective buffering capacity is exceeded, the pH values of both subsystems shift in the same direction.

From an applied point of view, the concept of collective buffering action may have implications for environmental monitoring. Traditional monitoring programs focus on soil and groundwater separately. Our results demonstrate that their joint assessment provides an earlier indication of acid-base disturbances. Monitoring the negative correlation phase, in particular, can serve as a sensitive early warning signal of destabilization before irreversible shifts occur.

References

- Fabian, C., Reimann, C., Fabian, K., Birke, M., Baritz, R., & Haslinger, E. (2014). GEMAS: Spatial distribution of the pH of European agricultural and grazing land soil. *Applied Geochemistry*, 48, 207–216. <https://doi.org/10.1016/j.apgeochem.2014.07.017>.
- Hájek, M., Jiménez-Alfaro, B., Hájek, O., Brancaloni, L., Cantonati, M., Carbognani, M., Dedić, A., Dítě, D., Gerdol, R., Hájková, P., Horsáková, V., Jansen, F., Kamberović, J., Kapfer, J., Kolari, T., Lamentowicz, M., Lazarević, P., Mašić, E., Moeslund, J.E., Pérez-Haase, A., Peterka, T., Petraglia, A., Pladevall-Izard, E., Plesková, Z., Segadelli, S., Semeniuk, Y., Singh, P., Šimová, A., Smerdová, E., Tahvanainen, T., Tomaselli, M., Vystavna, Y., Biță-Nicolae, C., & Horsák, M. A. (2021). European map of groundwater pH and calcium. *Earth System Science Data Discussions*, 13(3), 1089–1105. <https://doi.org/10.5194/essd-13-1089-2021>.
- Hillel, D. (2004). *Introduction to environmental soil physics*. Elsevier Academic Press, 494 p.
- Kida, K., & Kawahigashi, M. (2015). Influence of asphalt pavement construction processes on urban soil formation in Tokyo. *Soil Science and Plant Nutrition*, 61, 135–146. <https://doi.org/10.1080/00380768.2015.1048182>.
- Klaus, M. (2023). Decadal increase in groundwater inorganic carbon concentrations across Sweden. *Communications Earth & Environment*, 4, 221. <https://doi.org/10.1038/s43247-023-00885-4>.
- Lewis, E., & Wallace, D.W.R. (1998). Program developed for CO_2 system calculations. Technical Report. <https://doi.org/10.2172/639712>.
- Luo, W.T., Nelson, P.N., Li, M.-H., Cai, J.P., Zhang, Y.Y., Zhang, Y.G., Yang, S., Wang, R.Z.Z., Wang, W., Wu, Y.N., Han, X.G., & Jiang, Y. (2015). Contrasting pH buffering patterns in

- neutral-alkaline soils along a 3600 km transect in northern China. *Biogeosciences*, 12, 7047—7056. <https://doi.org/10.5194/bg-12-7047-2015>.
- Nelson, P.N., & Su, N. (2010). Soil pH buffering capacity: a descriptive function and its application to some acidic tropical soils. *Australian Journal of Soil Research*, 48, 201—207. <https://doi.org/10.1071/SR09150>.
- Plummer, L.N., & Busenberg, E. (1982). The solubilities of calcite, aragonite and vaterite in CO₂-H₂O solutions between 0 and 90 °C, and an evaluation of the aqueous model for the system CaCO₃-CO₂-H₂O. *Geochimica et Cosmochimica Acta*, 46(6), 1011—1040. [https://doi.org/10.1016/0016-7037\(82\)90056-4](https://doi.org/10.1016/0016-7037(82)90056-4).
- Sasidhar, V., & Ruckenstein, E. (1981). Electrolyte osmosis through capillaries. *Journal of Colloid and Interface Science*, 82, 439—457. [https://doi.org/10.1016/0021-9797\(81\)90386-6](https://doi.org/10.1016/0021-9797(81)90386-6).
- Slessarev, E.W., Lin, Y., Bingham, N.L., Johnson, J.E., Dai, Y., Schimel, J.P., & Chadwick, O.A. (2016). Water balance creates a threshold in soil pH at the global scale. *Nature*, 540, 567—569. <https://doi.org/10.1038/nature20139>.
- Stumm, W., & Morgan, J.J. (1996). *Aquatic chemistry: chemical equilibria and rates in natural waters*. New York: Wiley-Interscience, 1040 p.
- Zhovinsky, E.Ya., Kuraeva, I.V., Kryuchenko, N.O., & Dmytrenko, G.E. (2001). Geology-structural and geochemical conditions of formation of fluorine-bearing provinces of Ukraine. *Mineralogical Journal*, 23(5/6), 31—36.

Вивчення кислотно-лужного балансу в системі ґрунт—підземні води

О.А. Хахель¹, Т.П. Ромашко², 2026

¹Полтавська гравіметрична обсерваторія Інституту геофізики ім. С.І. Субботіна НАН України, Полтава, Україна

²Полтавський державний аграрний університет, Полтава, Україна

Взаємодія між системами рН-буфера ґрунту та підземних вод може відігравати певну роль у формуванні гідрогеохімічних умов, що впливають на стабільність рН у цих двох середовищах. Незважаючи на широкі дослідження ґрунту та підземних вод, пов'язана поведінка цих систем залишається недостатньо вивченою, особливо в умовах просторової гетерогенності та антропогенного впливу. Ця робота має на меті вивчити взаємодію між механізмами буфера рН ґрунту та хімією підземних вод, зосереджуючись на визначенні домінуючих процесів, що керують регуляцією рН, шляхом вимірювання рН, загальної лужності, концентрації іонів кальцію та компонентів карбонатної буферної системи. Ґрунт та підземні води показали взаємопов'язаний буферний механізм. Стабілізація рН у досліджуваній системі контролюється комбінованим впливом кількох буферних механізмів, включаючи мінеральну рівновагу, іонний обмін та реакції у розчинній фазі. Аналіз показує, що ці процеси діють пов'язано та залежать від гідродинамічних умов та місцевих факторів навколишнього середовища. Запропоновано концептуальну модель «колективної буферної дії» для опису інтегрованого ефекту взаємодіючих буферних процесів, завдяки яким ґрунти та ґрунтові води функціонують як інтегрована кислотно-лужна система. Модель призначена для якісної інтерпретації, радше ніж для повного кількісного представлення. Було визначено три фази буферної взаємодії між ґрунтом та ґрунтовими водами, починаючи від фонові рівноваги до розвиненого підлужування або підкислення, з протилежними або синхронізованими зрушеннями рН ґрунту та ґрунтових вод залежно від фази. Цей механізм може служити раннім індикатором попередження порушень кислотно-лужного балансу та має практичне значення для гідрологічного моніторингу навколишнього середовища.

Ключові слова: рН ґрунту, рН ґрунтових вод, взаємодія рН-буферів.